

the LV unipolar lead with appropriate sensing, impedance, and capture thresholds with the new RV lead.

**Conclusion:** This patient was referred for system revision for inadequate sensing on her ICD lead, however, after DFTs we determined that she had suffered a conductor fracture in the lead, which also raised questions about her unipolar epicardial LV lead. Revision of the RV lead, although not for the original problem prompting referral, fixed her system.

## B-PO03-016

### DISEASE-ASSOCIATED CALMODULIN VARIANTS INTERACTION WITH THE KCNQ1 POTASSIUM CHANNEL

Po Wei Kang MSE, Paweom Angsutararux, Jingyi Shi PhD, Martina Marras, Carlota Abella, Jianmin Cui PhD and Jonathan Silva PhD

**Background:** Calmodulin (CaM) is a ubiquitous auxiliary subunit and a potent modulator of key ion channels underlying the cardiac action potential (AP). Patients carrying CaM variants often present early in life with severe arrhythmia. Mechanisms by which CaM variants lead to arrhythmias are complex, given that CaM regulates myriad ion channels. One prominent CaM regulatory target is the KCNQ1 voltage-gated potassium channel, which is responsible for the key repolarizing  $I_{Ks}$  current. Despite CaM serving as an obligatory subunit for KCNQ1, relatively little is known regarding how disease-associated CaM variants might affect KCNQ1 function. Here, we present fluorescence and electrophysiological results characterizing disease-associated CaM variants interaction with KCNQ1.

**Objective:** To understand whether KCNQ1 channel dysfunction arising from aberrant interaction with disease-associated CaM variants may contribute to arrhythmogenesis.

**Methods:** We employed live-cell fluorescence resonance energy transfer (FRET) to quantify binding interaction for the first time between KCNQ1 channels and disease-associated human CaM variants. CaM variants were further assayed by voltage clamp to characterize potential aberration in ionic current conductance.

**Results:** Live-cell FRET assay revealed CaM variants with lower (e.g. CaM Q136P) or similar (e.g. CaM F142L) binding affinity to KCNQ1 compared to wild-type CaM. As CaM binding is required for KCNQ1 assembly, CaM variants with diminished binding affinity to KCNQ1 will likely impede KCNQ1 membrane trafficking, resulting in a Long QT phenotype. CaM variants with wild-type level binding affinity to KCNQ1 likely permit channel expression but may induce abnormal current. CaM F142L binds KCNQ1 with higher affinity compared to wild-type, but exerts minor functional changes to KCNQ1 current with or without KCNE1 co-expression. The pathology associated with the CaM F142L variant is not likely due to interaction with KCNQ1.

**Conclusion:** Our results delineate which CaM disease variants induce aberrant interaction with KCNQ1 and for the first time provide a method to quantify how altered CaM-KCNQ1 binding affinity plays a role in arrhythmogenesis associated with human CaM variants.

## B-PO03-017

### ROLE OF $K_{V11.1}$ MISTRAFFICKING IN HIGHLY PENETRANT *KCNQ1* VARIANTS

Yuko Wada MD, PhD, Andrew M. Glazer PhD, Ayesha Muhammad, Tao Yang, Laura L. Short, Lynn D. Hall and Dan M. Roden MD, FHRS

**Background:** Loss of function (LOF) variants in *KCNQ1* or *KCNH2*, encoding  $K_{V7.1}$  and  $K_{V11.1}$  respectively, are the commonest causes of the congenital long QT syndrome (LQTS). Previous studies have suggested that a  $K_{V7.1}$ - $K_{V11.1}$  interaction can modulate  $K_{V11.1}$  cell surface expression and

thus determine whether a *KCNQ1* LOF variant generates a severe phenotype.

**Objective:** To define mechanisms whereby haploinsufficient (HI) *KCNQ1* variants can nevertheless generate a severe LQTS phenotype.

**Methods:** We studied induced pluripotent stem cell-derived cardiomyocytes (iPSC-CMs) from a patient with Jervell Lange-Nielsen syndrome (JLN) caused by biallelic LOF variants of *KCNQ1*: R518X (known to cause nonsense-mediated mRNA decay) and an exon6 skipping splicing variant ( $ex6_{skip}$ ).  $I_{Kr}$  and  $I_{Ks}$  were compared in JLN cells before and after R518X was corrected by genome editing, and to control cells. We also generated stable HEK293 lines expressing both wild-type *KCNH2* and *KCNQ1* wild-type,  $ex6_{skip}$ , or one of 5 HI clinically highly penetrant *KCNQ1* variants: F340del, A341V, T587M, R591H, R594Q. We quantified  $K_{V11.1}$  surface abundance by flow cytometry and assessed  $K_{V7.1}$ - $K_{V11.1}$  interactions by co-immunoprecipitation (co-IP).

**Results:** JLN iPSC-CMs showed prolonged action potentials and near total loss of  $I_{Ks}$ . In edited cells carrying only  $ex6_{skip}$ ,  $I_{Ks}$  was significantly increased ( $0.1 \pm 0.03$  pA/pF to  $1.3 \pm 0.3$  pA/pF [mean  $\pm$  S.E.] at 40 mV) compared to control ( $0.9 \pm 0.4$  pA/pF), but  $I_{Kr}$  was significantly decreased ( $1.9 \pm 0.2$  to  $0.2 \pm 0.1$  pA/pF at 20 mV; control =  $1.4 \pm 0.2$  pA/pF). In HEK293 co-IP experiments, F340del, A341V, and  $ex6_{skip}$  produced no  $K_{V7.1}$  and no  $K_{V11.1}$  binding while the other variants (R591H, T587M, R594Q) did generate  $K_{V7.1}$  which interacted with  $K_{V11.1}$ . Despite these differences, all 6 variants decreased  $K_{V11.1}$  surface abundance, by 8-22%, compared to wild-type.

**Conclusion:** Penetrant HI variants decrease  $K_{V11.1}$  surface abundance through multiple mechanisms. These data reinforce the importance of assessing not only  $I_{Ks}$  alone but also  $I_{Kr}$  as mediators of disease severity in LQTS.

## B-PO03-018

### CLINICAL CHARACTERISTICS AND ELECTROPHYSIOLOGIC PROPERTIES OF *SCN5A* VARIANTS IN FEVER-INDUCED BRUGADA SYNDROME

Ganxiao Chen MD, Hector Barajas-Martínez PhD, FHRS, Hao Xia MD, PhD, Bian Li PhD, John A. Capra PhD, Ryan Pfeiffer BS, Kai Guo MD, PhD, Zhonghe Zhang MD, Xiu Chen MD, Bo Yang MD, PhD, Hong Jiang MD, PhD, Yaxun Sun MD, PhD, Gary Tse, Chloe Miu Mak MD, PhD, Yoshiyasu Aizawa MD, PhD, FHRS, Michael H. Gollob MD, PhD, FHRS, Charles Antzelevitch PhD, FHRS and Dan Hu MD, PhD, FHRS

**Background:** Brugada syndrome (BrS) is a severe inherited arrhythmia syndrome which can be unmasked by fever.

**Objective:** To describe the clinical features and unique characteristics of *SCN5A* mutations contributing to the development of fever-induced BrS.

**Methods:** The clinical analysis was performed in 134 probands diagnosed with fever-induced BrS, including 59 patients who received next-generation genetic sequencing. We employed a biophysics-based computational protocol to investigate whether protein structure destabilization contributes to Nav1.5 variant-mediated fever-induced BrS.

**Results:** Among all cases enrolled, the symptoms at diagnosis were syncope in 26 (19.40%) and major arrhythmic events (MAE) in 16 (11.94%). *SCN5A* variant carriers were significantly younger than probands free of *SCN5A* variants. Multivariate analysis indicated that younger age, Caucasian ethnicity, family history of SCD, and wider Tpeak-Tend interval were independent predictors of MAE. Compared with a historical cohort of non-fever BrS probands carrying *SCN5A* variants, carriers with fever-induced BrS were prone to MAE at a younger age, and had a

higher proportion of variants localizing at the interdomain linkers. Modeling result showed that most variants are destabilizing when temperature increases, suggesting that Nav1.5 structure destabilization is the cause of fever-induced BrS associated with SCN5A variants.

**Conclusion:** In our cohort, SCN5A variant carriers with fever-induced BrS present at a younger age and harbor SCN5A variants predominantly localized to interdomain linker regions of Nav1.5. These SCN5A variants typically induce destabilization of Nav1.5 structure at higher body temperatures. Patients with SCN5A mutations present within interdomain linker regions may warrant more aggressive monitoring and management of fever.

## B-PO03-019

### CARDIAC CONTRACTILITY MODULATION STIMULATION DURING SYSTOLE ENHANCES CONTRACTION AND CALCIUM HANDLING PROPERTIES IN HUMAN-INDUCED PLURIPOTENT STEM CELL-DERIVED CARDIOMYOCYTES

T.K. Feaster PhD, Maura Casciola PhD, Akshay Narkar PhD and Ksenia Blinova PhD

**Background:** Cardiac contractility modulation (CCM) is a cardiac therapy whereby non-excitatory electrical simulations are delivered to the heart during the absolute refractory period. We previously evaluated effects of CCM and found adult rabbit cardiomyocytes display a transient increase in calcium and contractility.

**Objective:** In the present study, we sought to extend these results to human stem-cell cardiomyocytes (hiPSC-CMs).

**Methods:** hiPSC-CMs (iCell Cardiomyocytes<sup>2</sup>, Fujifilm Cellular Dynamic Inc) were studied in monolayer format on Matrigel mattress substrate. Contractility, calcium and electrophysiology were evaluated by image and fluorescence analysis (CellOPTIQ, Clyde Biosciences). Standard clinical CCM pulse parameters were applied with an A-M Systems 4100 pulse generator (Figure 1).

**Results:** Robust CCM response was observed at 11 V/cm (64 mA) for pacing and 22 V/cm (128 mA) for CCM. The first CCM beat displayed a  $19.7 \pm 0.03\%$ , (\*\*P<0.01, n=10) contraction amplitude increase that reached steady-state within 5 beats at  $8.3 \pm 0.16\%$ . CCM stimulation resulted in faster contraction and relaxation kinetics of  $25.9 \pm 0.07\%$  and  $18.6 \pm 0.07\%$  respectively. Likewise, calcium amplitude increased by  $59.3 \pm 0.03\%$  (\*P<0.05, n=3).

**Conclusion:** This study provides a comprehensive characterization of the effects of CCM on hiPSC-CMs. These data suggest, CCM exerts its effects by, at a minimum, two calcium centric mechanisms including 1) modulation of L-type calcium channels and 2) increased myofilament calcium sensitivity. These data provide the first study of CCM in hiPSC-CMs and demonstrates the utility of hiPSC-CMs to evaluate safety and effectiveness of cardiac medical devices.

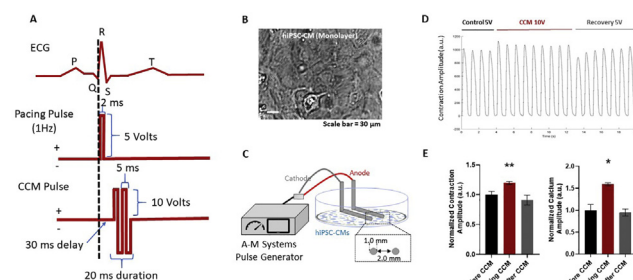


Figure 1. (A) Standard clinical CCM pulse parameters. (B) Representative images of hiPSC-CM monolayer (C) Schematic representation of CCM device setup with platinum electrodes in 1 well of a 48-well plate. (D) Representative contraction trace control SV, 4 beats (0 – 4 sec), CCM 10 V, 9 beats (4 – 13 sec), Recovery SV, 7 beats (13 – 20 sec) displaying increased amplitude and kinetics induced by CCM. (E) Summary data Mean  $\pm$  SEM N = 3 – 10, for the last control beat, first CCM beat, and first recovery beat. \*\*P<0.01, \*P<0.05.

## B-PO03-020

### BECLIN-1 DEFICIENCY IN MESENCHYMAL STROMAL CELLS (MSCS) WITH DESMOPLAKIN MUTATIONS ENHANCES THE ACTIVATION OF PROFIBROGENIC GENES BY TGF- $\beta$ 1 VIA THE P38 MAPK SIGNALING PATHWAY

Shing Fai Chan PhD, Ardan Saguner MD, Corinna B. Brunckhorst MD, Chuanyu Wei, Firat Duru MD, Joseph E. Marine MBA, MD, FHRS, Cynthia A. James PhD, CGC, Hugh Calkins MD, FHRS, Daniel P. Judge MD and Hwei-Sheng V. Chen MD, PhD

**Background:** Among desmosome gene mutations in arrhythmogenic cardiomyopathy (AC), desmoplakin (*DSP*) mutations appear to induce aggressive fibrosis preceding left ventricular dysfunction in AC hearts. MSCs are the progenitor cells for myofibroblasts responsible for fibrogenesis. In normal MSCs, transforming growth factor beta-1 (TGF- $\beta$ 1) induces transient activation of both profibrogenic genes and autophagy that limit collagen production to normal reparative responses. We previously showed that *DSP* mutations cause reduction in both wild-type (WT) *DSP* levels and availability of beclin-1 (*BECN1*), an essential mediator of autophagy, in MSCs (*BECN1* deficiency). Increased vimentin-*BECN1* binding accounted for this *BECN1* deficiency, which decreased autophagy and enabled collagen accumulation/secretion after TGF- $\beta$ 1.

**Objective:** Further elucidation of pathogenic mechanisms by which *DSP* mutations trigger aggressive fibrosis in AC may enable developing novel therapies.

**Methods:** We generated iPSC-derived MSCs from normal individuals and 2 unrelated AC patients with *DSP* c.478C>T (p. Arg160X) or *DSP* c.3474\_3475insA (p. Glu1159Argfs\*3) mutations. We studied the fibrogenic responses of these MSCs to 3 days of TGF- $\beta$ 1 treatment using standard Western/Co-IP, autophagy flux assay, immunostaining, and qPCR.

**Results:** Compared to normal MSCs, mutant *DSP* MSCs showed exaggerated collagen accumulation/secretion, and 2.0- to 3.4-fold of over-activation of profibrogenic genes at day 3 after TGF- $\beta$ 1 [ $\sim$ 2.8-fold in collagen 1a1 (*COL1A1*),  $\sim$ 3.4-fold in collagen 3a1 (*COL3A1*), and 2.0-fold in fibronectin (*FN*)], consistent with enhanced profibrogenic responses. We show here that hyperactivation of *COL1A1*, *COL3A1* and *FN* genes by TGF- $\beta$ 1 in mutant *DSP* MSCs is mediated by over-activated p38 pathways due to *BECN1* deficiency, which could be reversed by a p38 inhibitor or *BECN1* overexpression.

**Conclusion:** We show for the first time that *DSP* mutations lead to decreased WT *DSP* levels and *BECN1* deficiency, resulting in excessive accumulation of collagen from decreased autophagy, and profibrogenic gene hyperactivation from over-activated p38 signaling after TGF- $\beta$ 1.

## B-PO03-021

### A MODEL PREDICTING LESION EXTENT FOR PULSED FIELD ABLATION

James Eason, Borna Sobati BS, David Clague PhD and Christopher P. Porterfield MD, MPH

**Background:** Ablation using pulsed fields (PF) reduces the likelihood of peripheral tissue damage arising from thermal ablation techniques. We have developed a novel simulation model that accurately predicts the extent of lesion formation in myocardial tissue from PF.

**Objective:** We aim to describe the mechanism of lesion formation in myocardial tissues and identify the waveform characteristics that maximize lesion extent as a function of delivered energy.